

**Cell Systems, Volume 11**

## **Supplemental Information**

### **Pairwise Stimulations of Pathogen-Sensing Pathways**

#### **Predict Immune Responses**

#### **to Multi-adjuvant Combinations**

**Surya Pandey, Adam Gruenbaum, Tamara Kanashova, Philipp Mertins, Philippe Cluzel, and Nicolas Chevrier**

Figure S1

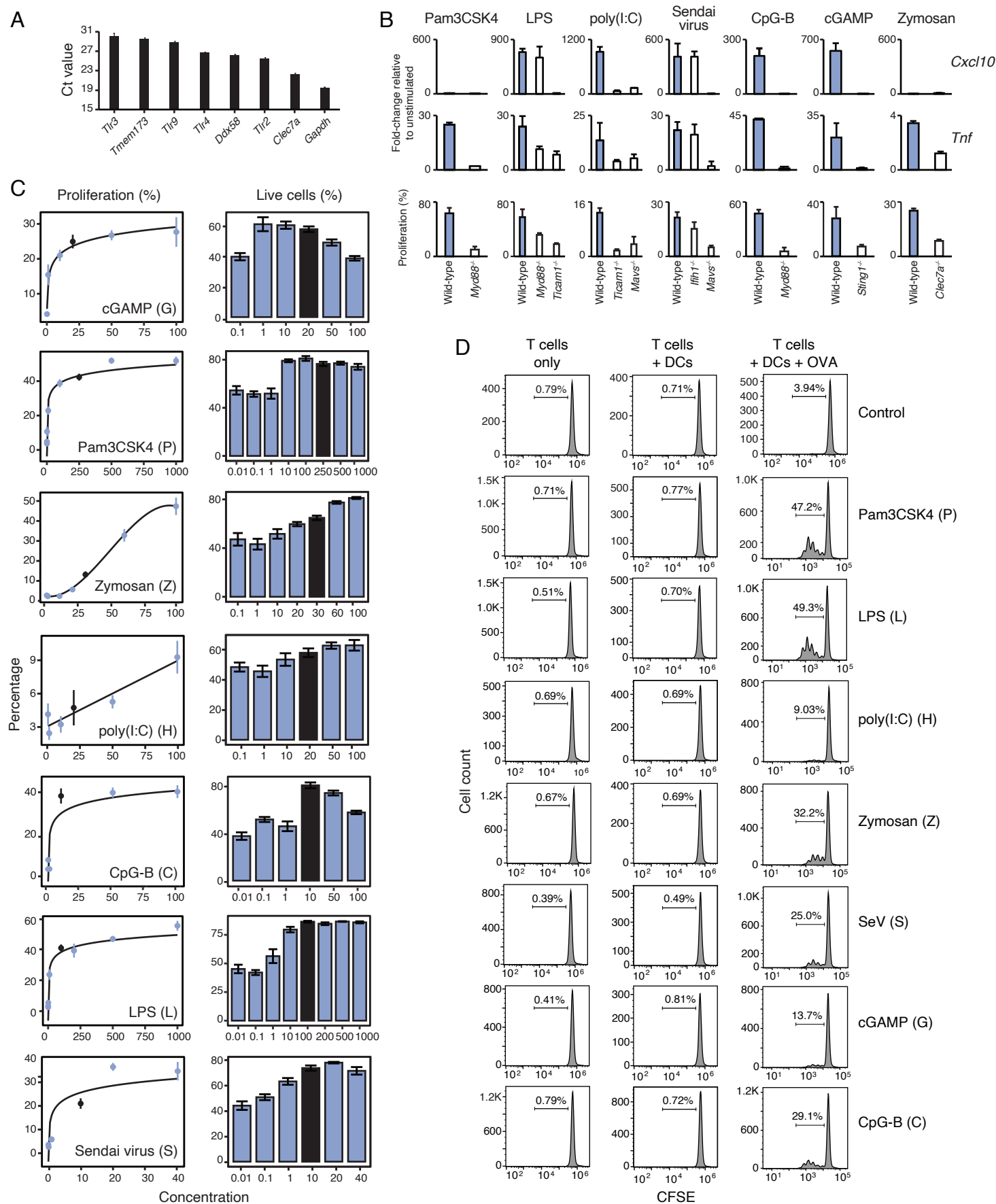


### Figure S1. Selection of pattern-recognition receptor ligands, Related to Figure 1

(A) Bar graph showing steady state mRNA expression in mouse dendritic cells (DCs) of the pattern recognition receptors or adaptor encoded by the following genes: *Tlr4*, *Tlr2*, *Tlr3*, *Tlr9*, *Ddx58* (RIG-I), *Clec7a* (DECTIN-1) and *Tmem173* (STING), which collectively recognize the seven ligands used in this study. Error bars, SD ( $n = 2$ ).

(B) Bar graphs showing mRNA expression of *Cxcl10* and *Tnf* (top two rows) and OT-II T cell proliferation (bottom row) upon stimulation of wild type (WT) and indicated knockout mouse dendritic cells (DCs) with the seven ligands selected for this study: cGAMP, CpG-B, Pam3CSK4, LPS, Zymosan, Sendai virus and poly(I:C). Error bars, SD ( $n = 2$ ).

(C) Dose-response analysis for the seven ligands selected for this study (indicated in left plots). For each ligand, indicated concentrations were used to stimulate DCs prior to adding OT-II cells ( $\mu\text{g/mL}$  for ligands G, Z, H, C and S;  $\text{ng/mL}$  for ligands P and L). Shown are proliferation (line plots; left) and viability (bar plots; right) measurements for OT-II T cells as a function of ligand concentrations. For proliferation plots, the logarithmic (G, C, P, L and S), linear (H) and cubic (Z) fits are shown as solid lines. The black circles (proliferation plots) and bars (viability plots) indicate the concentration selected for combinatorial screening analyses. Error bars, SEM ( $n = 3$ ).

(D) To control for the potential effects of ligands on T cells, as opposed to DCs, we measured OT-II T cells proliferation with CFSE in three conditions using indicated ligands: (1) T cells incubated with ligands only (T cells only; left), (2) T cells incubated with DCs that were stimulated and washed prior to the addition of T cells (T cells + DCs; middle), and (3) T cells incubated with DCs that were stimulated, pulsed with the ovalbumin protein and washed prior to the addition of T cells (T cells + DCs + Ovalbumin; right). Shown are representative CFSE profiles from live OT-II  $\text{CD4}^+$  T cells ( $n = 3$ ).

Figure S2

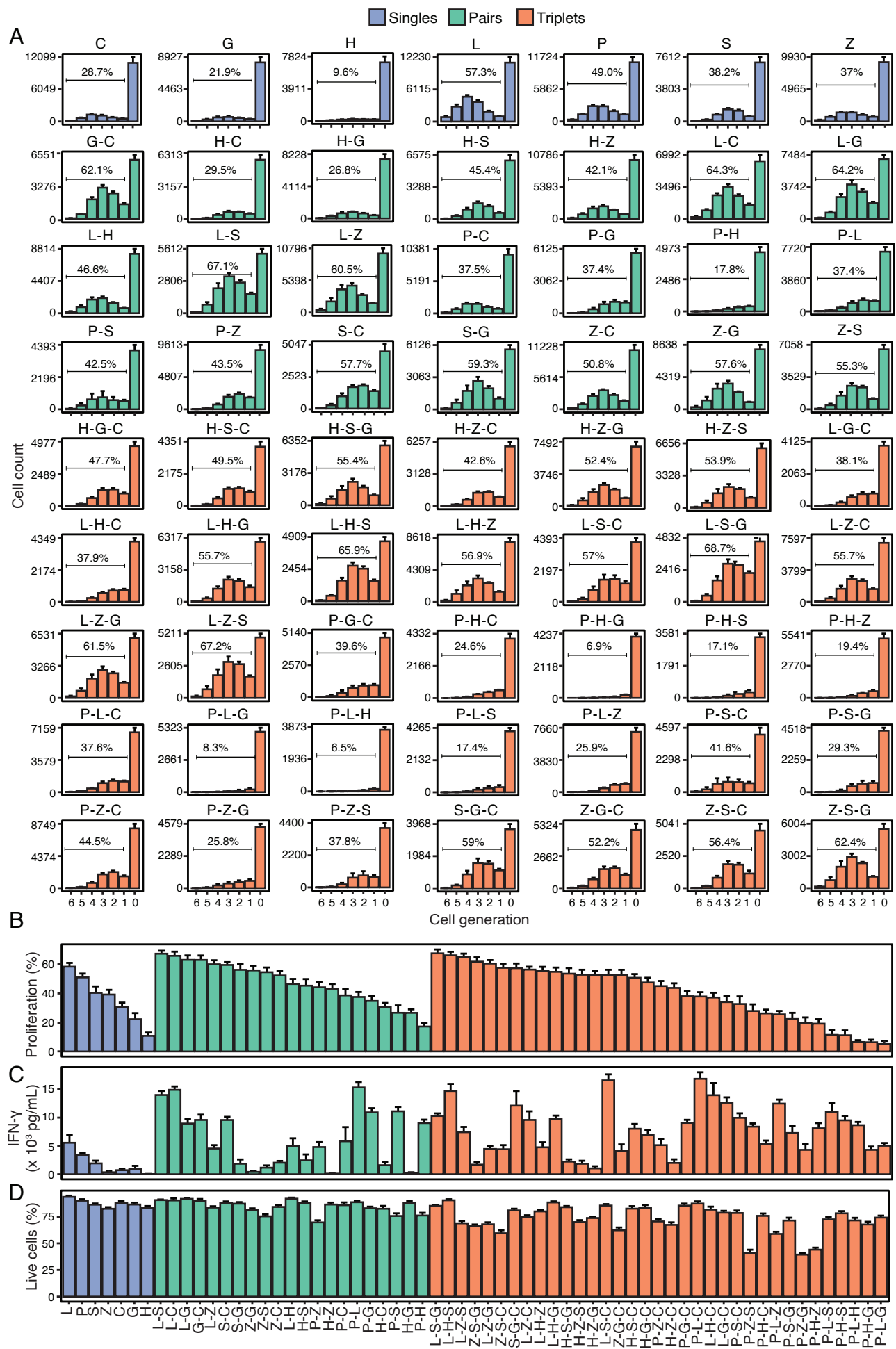


**Figure S2. Impact of combinatorial stimulations of dendritic cells on T cell proliferation, cytokine secretion and viability, Related to Figure 1**

(A) Bar plots showing the CFSE profiles of OT-II cells cocultured with DCs stimulated with indicated ligand singles (blue), pairs (green) and triplets (orange). Percentages show the proportion of cells that underwent division. Error bars, SEM ( $n = 8$ ).

(B-D) Bar plots showing the proportion of OT-II cells that divided (B), the production of IFN- $\gamma$  in DC-OT-II coculture supernatants (C), and the percentage of live OT-II cells (D) upon DC stimulations with indicated ligand singles (blue), pairs (green) and triplets (orange). Error bars, SEM ( $n = 8$ ).



**Figure S3. Pairwise and triplet interaction scoring across triplets of stimuli, Related to Figure 2**

Line plots showing the number of OT-II cells in each generation of activated cells (cell generation 1 to 6) upon coculture with DCs stimulated with singles (blue) and pairs (green) corresponding to indicated triplets (top). Bar plots indicate pairwise ( $I_{AB} = P_{iAB} - P_{iA}P_{iB}$ ) and triplet ( $I_{ABC} = P_{iABC} - P_{iA}P_{iB}P_{iC}$ ) interaction scores for indicated triplets and their composite pairs. Triplet scores are derived from  $P_{iABC}$  values observed experimentally (orange) or calculated (white) using the Isserlis formula:  $P_{iABC} = P_{iAB}P_{iC} + P_{iAC}P_{iB} + P_{iBC}P_{iA} - 2P_{iA}P_{iB}P_{iC}$ . Shown are 32 out of the 35 triplets tested, with the remaining 3 shown in Figure 2A-C, ordered by decreasing triplet interaction scores (as in Figure 2E). Error bars, SEM ( $n = 8$ ).

Figure S4

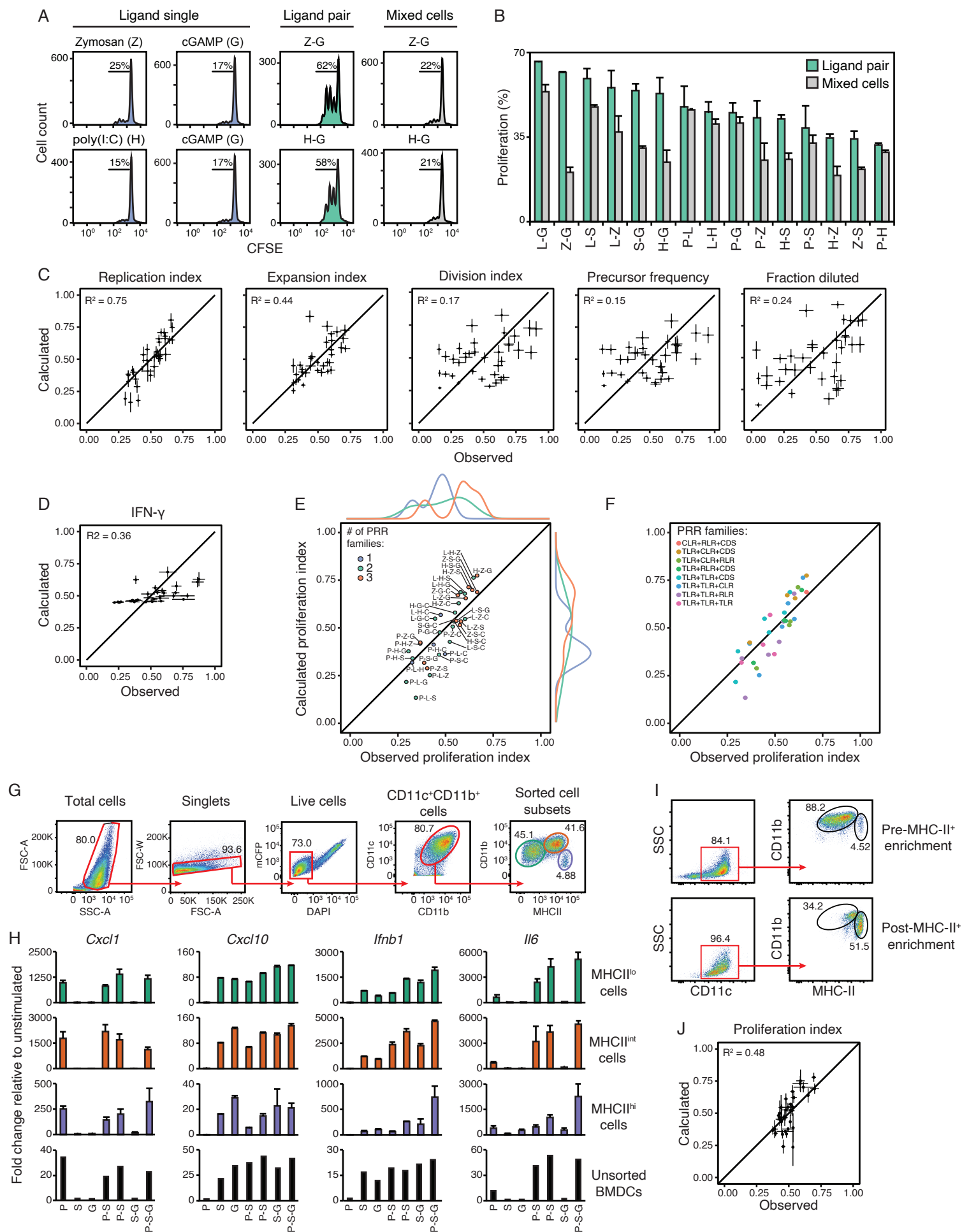




**Figure S4. Assessing various T cell proliferation metrics and the clustering of ligand triplets and their proliferation in relationship to receptor families, Related to Figure 3**

(A) CFSE profiles of OT-II CD4<sup>+</sup> T cells cocultured with DCs stimulated with indicated ligand singles, ligand pairs, or DCs stimulated with ligand singles and mixed at 1:1 ratio (Mixed cells). Percentages show the proportion of cells that underwent division.

(B) Bar plots showing the proportion of OT-II cells that divided in cocultures with DCs stimulated with indicated ligand pairs or DCs mixed after single ligand stimulations (Mixed cells). Error bars, SD ( $n = 3$ ).

(C-D) Dot plots of the observed (X axis) and calculated (Y axis) triplet values for all 35 ligand triplets tested and using the indicated CFSE-derived proliferation metrics (see STAR Methods) (C), or IFN- $\gamma$  concentrations from DC-OT-II cell cocultures (D). The solid line indicates  $y = x$ . Error bars, SEM ( $n = 8$ ). (E-F) Scatter plots of the observed (X axis) and calculated (Y axis) triplet proliferation index values for all 35 ligand triplets tested (same data as shown in Figure 3B). The solid lines indicate  $y = x$ . Colors indicate the number (E) and the type (F) of PRR families covered by a given triplet. CLR, C-type lectin receptor; TLR, Toll-like receptors; RLR, RIG-I-like receptor; CDS, cytosolic dsDNA sensor. In D, density distributions are shown (top and right) for the number of PRR pathways targeted by a ligand triplet: one, two and three PRR families per triplet.

(G-H) Gating strategy for fluorescence activated cell sorting (FACS) of the three following subpopulations present in GM-CSF-induced bone-marrow-derived DC cultures: CD11b<sup>+</sup>MHCII<sup>lo</sup> (green), CD11b<sup>+</sup>MHCII<sup>int</sup> (red), CD11b<sup>+</sup>MHCII<sup>hi</sup> (purple) cells (G), and qPCR analysis of *Cxcl1*, *Cxcl10*, *Ifnb1* and *Il6* gene expression in indicated subpopulations (right) stimulated with indicated ligand singles or combinations (P, Pam3CSK4; S, Sendai virus; G, cGAMP) (H). The bottom row in G indicates changes in gene expression measured by RNA-seq on total, unsorted BMDCs.

(I) Flow cytometry analysis of cells from total BMDC cultures before (top) or after (bottom) enrichment of MHC-II<sup>+</sup> cells using magnetic microbeads.

(J) Dot plots of the observed (X axis) and calculated (based on the Isserlis formula; Y axis) triplet proliferation index values for all 35 ligand triplets tested using MHC-II<sup>+</sup> DCs enriched as shown in I. The solid line indicates  $y = x$ . Error bars, SEM ( $n = 4-7$ ).

Figure S5

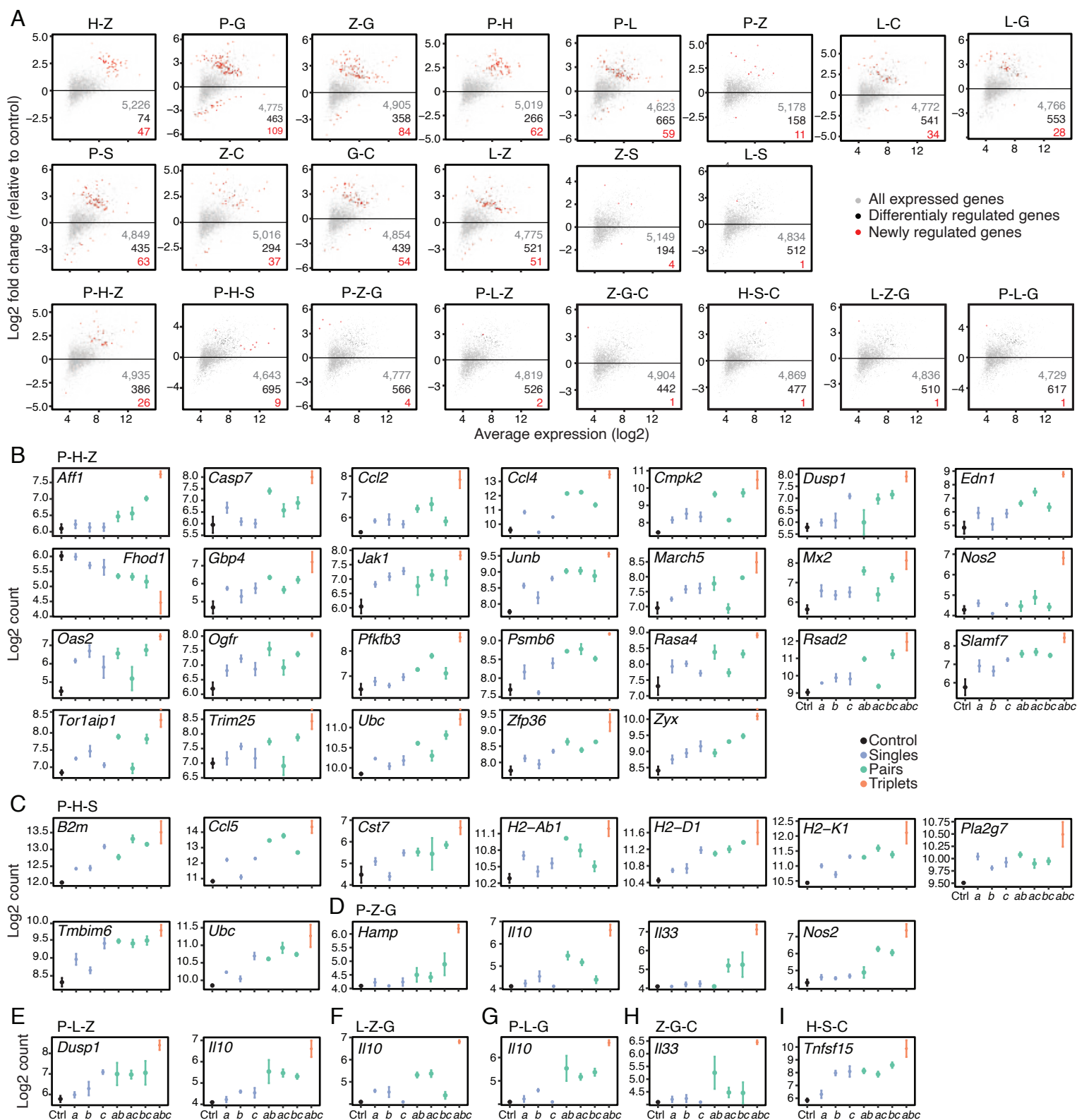


**Figure S5. Genes newly regulated by ligand pairs and triplets compared to their composite ligand singles and pairs, Related to Figure 4**

(A) Dot plots showing log<sub>2</sub> fold changes in gene expression (Y axis) in mouse DCs stimulated with indicated ligand pairs (14 out of 21 tested; top two rows) or triplets (8 out of 35 tested; bottom row) relative to unstimulated control cells against log<sub>2</sub> average expression values (X axis) ( $n = 3$ ). Red dots, genes regulated by indicated pairs or triplets but not by their composite ligand singles and/or pairs; black dots, all differentially regulated genes by indicated pairs or triplets; grey dots, all genes detected.

(B-I) Shown are normalized expression levels in mouse DCs for indicated genes as log<sub>2</sub> counts per million upon stimulation with indicated triplets: P-H-Z (B), P-H-S (C), P-Z-G (D), P-L-Z (E), L-Z-G (F), P-L-G (G), Z-G-C (H) and H-S-C (I). *a*, *b*, *c*, singles (blue dots); *ab*, *ac*, *bc*, pairs (green dots); *abc*, triplet (orange dots); Ctrl, control unstimulated cells (black dots). Error bars, SEM ( $n = 3$ ).

### Figure S6

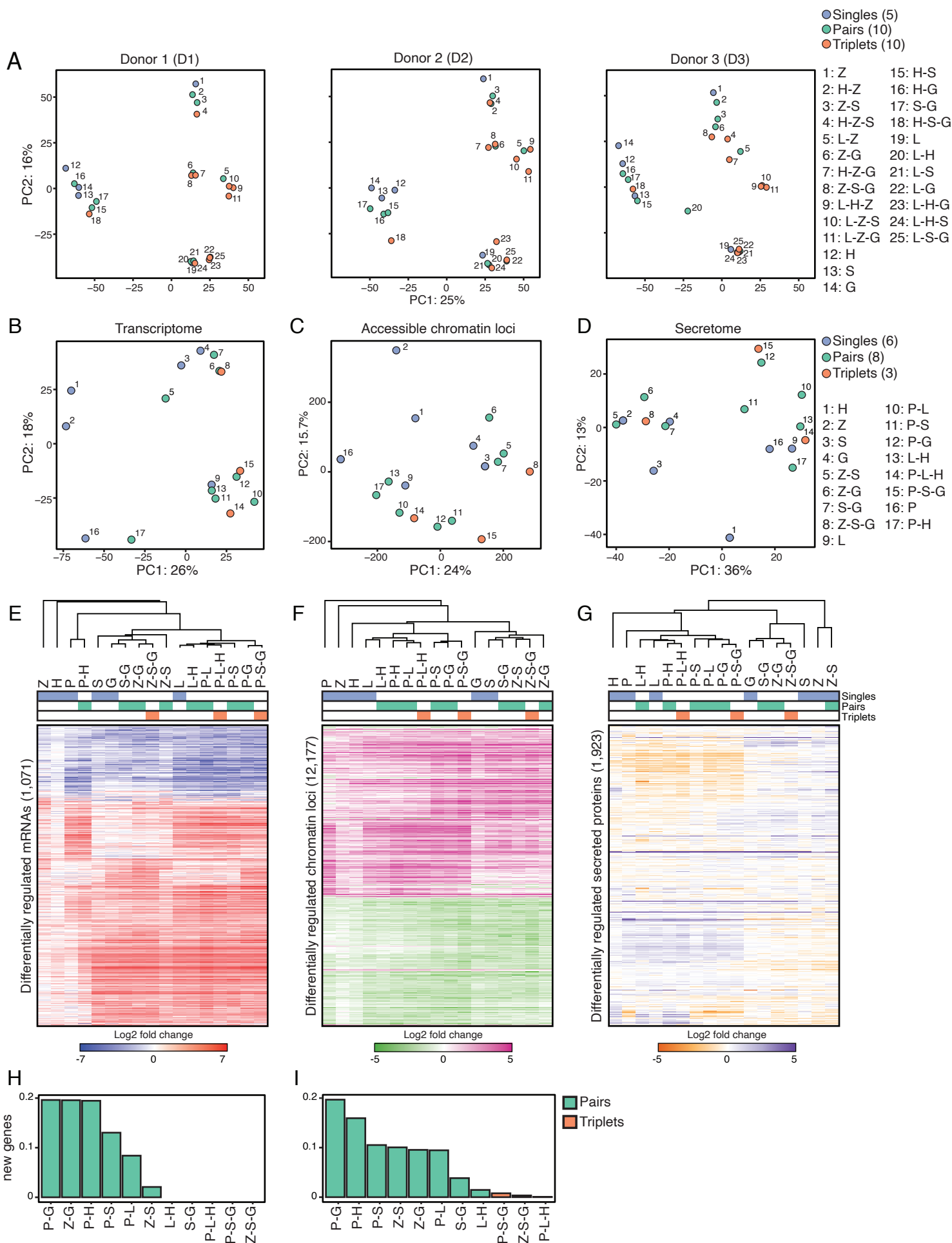


**Figure S6. Effects of combinatorial stimulations on the transcriptional, chromatin accessibility and secretome profiles of dendritic cells, Related to Figure 4**

(A) Principal component analysis (PCA) of mRNA profiles of human blood monocyte-derived DCs (moDCs) from three independent healthy donors (from left to right: donor (D) 1 to 3) stimulated with indicated ligand singles (5; blue), pairs (10; green) or triplets (10; orange).

(B-D) Principal component analysis (PCA) of mRNA (B), chromatin accessibility (C) and secretome (D) profiles of mouse DCs stimulated with indicated (numbers) ligand singles (6; blue), pairs (8; green) or triplets (3; orange) ( $n = 2-3$ ).

(E-G) Heatmaps of differentially regulated (rows) genes (E), accessible genomic loci (F), or secreted proteins (G) from mouse DCs stimulated with indicated ligand singles (6; blue), pairs (8; green) or triplets (3; orange). Values are log<sub>2</sub> fold-changes relative to unstimulated cells (color scales) ( $n = 2-3$ ).

(H-I) Bar plots showing for each ligand pair (green) or triplet (orange) the proportion of genes (H) or accessible loci (I) regulated by a triplet or pair but not by its composite ligand singles and/or pairs relative to the total number of genes (H) or loci (I) regulated by that triplet ( $n = 2-3$ ).

Figure S7

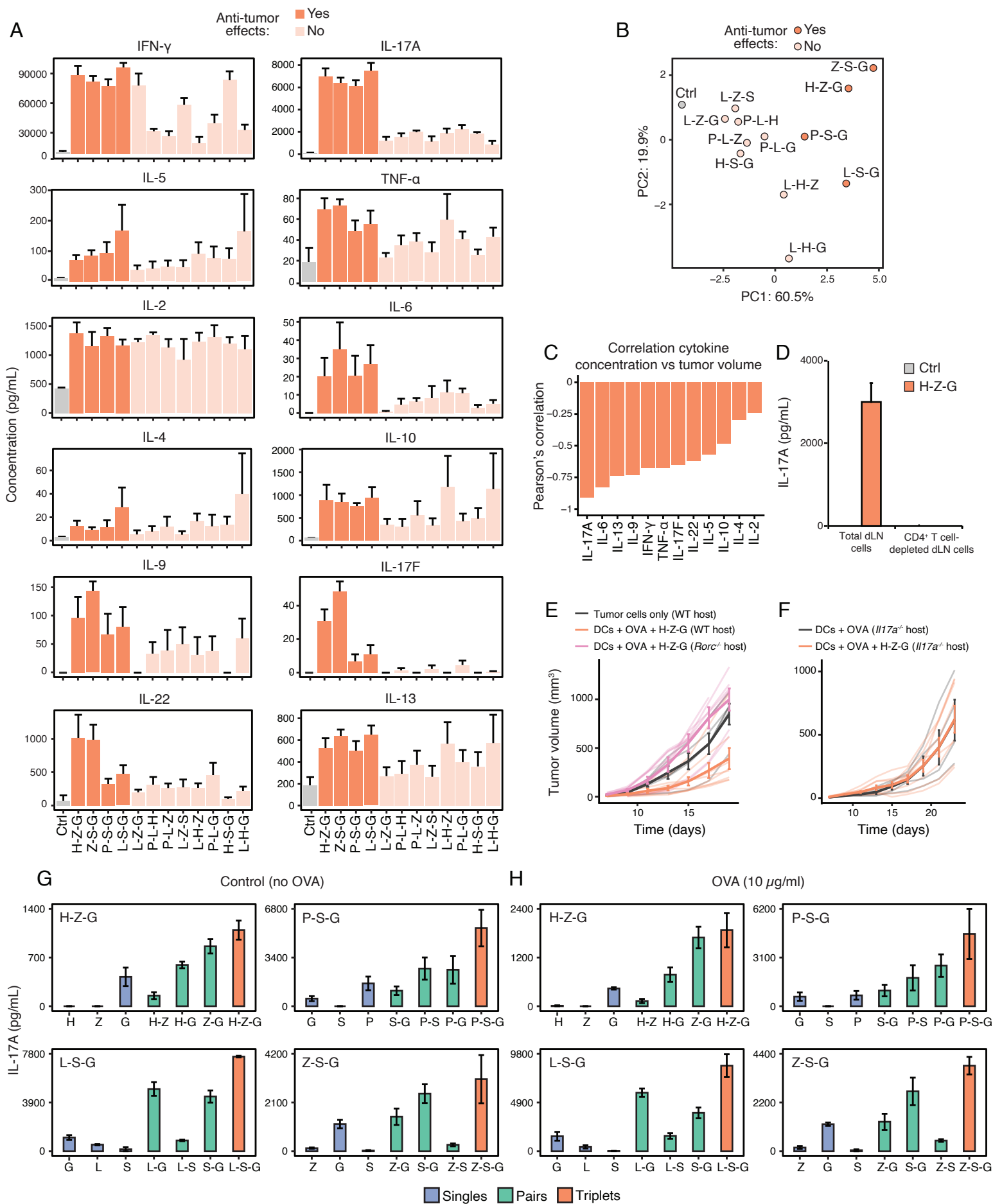


**Figure S7. Effects of DC vaccines on draining lymph node cytokine secretion profiles, Related to Figure 7**

(A-B) Bar plots (A) and principal component analysis (PCA; B) of the secretion profiles of 12 cytokines measured in supernatants from total draining lymph node (dLN) cell cultures upon *in vitro* restimulation with the OVA protein (1 µg/mL). dLN cells were prepared from mice injected a week earlier with DC vaccines pulsed with OVA and stimulated with indicated ligand triplets or left unstimulated as control (grey). Dark and light orange bars (A) and dots (B) respectively indicate ligand triplets with or without anti-tumor properties *in vivo* (based on data shown in Figure 5). Error bars, SEM ( $n = 4$ ).

(C) Pearson's correlation metric between cytokine concentrations (A) and B16-OVA tumor volumes at day 19 (Figure 5B) for the 12 adjuvant triplets used in tumor growth and dLN restimulation experiments.

(D) Production of IL-17A by total dLN cell cultures prepared from mice injected a week earlier with DC vaccines pulsed with OVA and stimulated with the H-Z-G (poly(I:C)-Zymosan-cGAMP) triplet (H-Z-G) or left unstimulated as control (Ctrl). Shown are results for total dLN cells (total dLN) and dLN cells depleted of CD4<sup>+</sup> T cells (CD4<sup>+</sup> T cell-depleted dLN cells).

(E-F) Mean tumor growth (solid lines) in cohorts of wild-type (WT), *Rorc*<sup>-/-</sup> and *Il17a*<sup>-/-</sup> knockout mice injected with 10<sup>5</sup> B16-OVA and indicated DC vaccines. DCs + OVA, unstimulated DCs pulsed with OVA; DCs + OVA + H-Z-G, DCs stimulated with H-Z-G and pulsed with OVA. Light color lines indicate tumor growth for individual mice within each cohort. Error bars, SEM ( $n = 3-6$  mice per cohort).

(G-H) IL-17A production by total inguinal draining lymph node (dLN) cells from mice injected subcutaneously with DC vaccines loaded with OVA and stimulated with indicated ligand singles or combinations covering the following four triplets with anti-tumor effects: H-Z-G, L-S-G, P-S-G and Z-S-G. dLN cells were plated 7 days post-DC vaccination in medium without OVA (G), or restimulated with 10 µg/mL of purified OVA protein (H). Blue, singles; green, pairs; orange, triplets. Error bars, SEM ( $n = 4$ ).